

# Titanium Phosphinidene and Phosphide Moieties from Oxidative Phosphorylation and Desilylation

Jacob S. Mohar, Mrinal Bhunia, Alexander L. Laughlin, Andrew Ozarowski, J. Krzystek, Taylor M. Keller, Michael R. Gau, Kyle M. Lancaster, Joshua Telser, and Daniel J. Mindiola\*



Cite This: <https://doi.org/10.1021/jacs.4c12242>



Read Online

ACCESS |

Metrics & More



Article Recommendations



Supporting Information

**ABSTRACT:** A unique entry into mononuclear titanium complexes bearing phosphinidene and phosphide ligand moieties is reported. Reaction of  $[K(\text{crypt})][(\text{PN})_2\text{TiCl}]$  (**1**, crypt = 2,2,2-cryptand) with  $[\text{Na}(\text{OCP})]$  results in  $[K(\text{crypt})][(\text{PN})_2\text{Ti}(\text{OCP})]$  (**2**) and such species can be oxidized to the derivative  $[(\text{PN})_2\text{Ti}(\text{OCP})]$  (**3**), both of which do not undergo decarbonylation. However, the reaction of **1** and  $[\text{NaP}(\text{SiMe}_3)_2]$  leads to an unprecedented  $\text{Ti}^{\text{III}}$  phosphinidene,  $[\text{K}(\text{crypt})][(\text{PN})_2\text{Ti}=\text{PSiMe}_3]$  (**4**), through an oxidative phosphorylation reaction. To promote the formation of a  $\text{Ti}\equiv\text{P}$  bond, complex **4** was treated with 0.5 equivalent  $\text{XeF}_2$ , resulting in an oxidative desilylation step forming a molecular titanium phosphide complex,  $[\text{K}(\text{crypt})][(\text{PN})_2\text{Ti}\equiv\text{P}]$  (**5**), which showed a characteristic downfield chemical shift at 1449.8 pmm in the  $^{31}\text{P}$  NMR spectrum. Complex **5** can be further functionalized to generate a terminal  $\text{Ti}^{\text{IV}}$  phosphinidene,  $[(\text{PN})_2\text{Ti}=\text{PSiMe}_3]$  (**6**), and the latter can be independently accessed through oxidation of **4**. All new complexes were characterized structurally and as appropriate by multinuclear NMR, CW X-band EPR (for  $\text{Ti}^{\text{III}}$ ), and HFEPR (for  $\text{Ti}^{\text{II}}$ ) spectroscopies.

Despite the growing utility of transition metal phosphide materials in electrochemistry and battery technologies,<sup>1–10</sup> only a handful of terminal, molecular, transition metal phosphidios ( $\text{M}\equiv\text{P}$ ) bearing a metal phosphorus triple bond have been isolated and structurally characterized.<sup>11–24</sup> Much of the early work regarding the synthesis of  $\text{M}\equiv\text{P}$  was established on group 6 metals (Mo and W) by Cummins, Schrock, and Scheer<sup>11–13,17,18,21</sup> utilizing  $\text{P}_4$  (Figure 1A)<sup>11–14,19</sup> and LiPHPh or  $\text{LiP}(\text{SiMe}_3)_2$  (Figure 1D)<sup>17,18,21</sup> as P atom transfer reagents. While these P atom sources enabled the synthesis of  $\text{M}\equiv\text{P}$  bonds to extend to group 5 metals (Nb) by Cummins<sup>14</sup> and Wolczanski,<sup>19</sup> it was not until a recent resurgence in the synthesis of other P atom transfer reagents<sup>25–30</sup> that  $\text{M}\equiv\text{P}$  bonding was extended to group 7 (Re) by Schneider<sup>22</sup> via decarbonylation of  $[\text{NaOCP}]$  or by Agapie via anthracene extrusion to form  $\text{Mo}^{\text{IV}}$  and  $\text{Mo}^{\text{V}}$  phosphides (Figure 1B,C). Despite these recent strides made in the synthesis of  $\text{M}\equiv\text{P}$  bonds, first row transition metals and group 4 metals remain underexplored. Group 4 elements pose an even greater challenge due to their propensity to have  $d^0$  valencies, the lack of suitable low-valent metal precursors, and low electronegativity (high energy d-orbitals), thus making it difficult for them to accept a  $\text{P}^{3-}$  fragment.<sup>31–35</sup> Due to our group's recent success in the synthesis of  $\text{Nb}\equiv\text{P}$ ,<sup>24</sup>  $[\text{Ti}\equiv\text{N}]^-$ ,<sup>31</sup> and more recently  $[\text{Ti}\equiv\text{As}]^-$  moieties,<sup>32</sup> we sought to synthesize a molecular example of a Ti-complex bound to a single P atom bearing a triple bond. In this study, we explore reactions of a  $\text{Ti}^{\text{II}}$  precursor  $[K(\text{crypt})][(\text{PN})_2\text{TiCl}]$ <sup>32</sup> (**1**), with  $[\text{Na}(\text{OCP})]$  and  $[\text{NaP}(\text{SiMe}_3)_2]$ , the latter of which allowed us to isolate an unprecedented  $\text{Ti}^{\text{III}}$  phosphinidene, a molecular  $\text{Ti}^{\text{IV}}$  phosphide, and its  $\text{Ti}^{\text{IV}}$  phosphinidene derivative (Figure 1).

Our first attempts at the synthesis of a  $\text{Ti}\equiv\text{P}$  moiety involved the use of the P atom transfer reagent  $[\text{Na}(\text{OCP})]$  given the analogous direct As-atom transfer from  $[\text{Na}(\text{OCAs})]$  to  $\text{Ti}^{\text{II}}$  to generate the first molecular  $[\text{Ti}\equiv\text{As}]^-$ .<sup>32</sup> Complex **1** reacts with  $[\text{Na}(\text{OCP})(\text{dioxane})_{2.5}]$  in THF at RT to yield  $[K(\text{crypt})][(\text{PN})_2\text{Ti}(\text{OCP})]$  (**2**) in 76% yield (Figure 2). In contrast to the reaction of **1** with  $[\text{Na}(\text{OCAs})]$ ,<sup>32</sup> **2** does not undergo decarbonylation likely in part due to the stronger P-CO bond as compared to the As-CO bond.<sup>33,34</sup> Compound **2** can be readily oxidized with  $[(\text{PN})_2\text{TiCl}]$  or  $[\text{FeCp}_2](\text{OTf})$  to generate  $[(\text{PN})_2\text{Ti}(\text{OCP})]$  (**3**, Figure 2) in 73% or 36% yield, respectively, along with formation of **1** or  $\text{FeCp}_2$  and  $\text{KOTf}$ .<sup>35</sup>

scXRD studies of **2** and **3** (Figure 3A,B) revealed the phosphaethynolate to be O-bound in each with a  $\text{Ti}-\text{O}$  bond of 2.070(3) (**2**; Figure 3A) and 1.978(2) (**3**; Figure 3B) Å. The decrease of ~0.092 Å from **2** to **3** is consistent with the decrease in atomic radius and increase in covalency from  $\text{Ti}^{\text{II}}$  (**2**) to  $\text{Ti}^{\text{III}}$  (**3**).<sup>36,37</sup> The geometry of **3** ( $\tau_s = 0.80$ ) is nearly identical with that of **2** ( $\tau_s = 0.77$ ) with O-binding of  $[\text{OCP}]^-$  being especially surprising since P-bound phosphaethynolate was proposed in low-valent Ti and isolated in  $\text{V}^{\text{III}}$ .<sup>39–42</sup> IR spectroscopy (KBr pellet) revealed vibrational stretching frequencies of  $\nu(\text{C}\equiv\text{P})$  as 1770 and 1655  $\text{cm}^{-1}$  for **2** and **3**, respectively,<sup>43</sup> and suggest the dominant resonance structure in

Received: September 4, 2024

Revised: March 11, 2025

Accepted: March 13, 2025

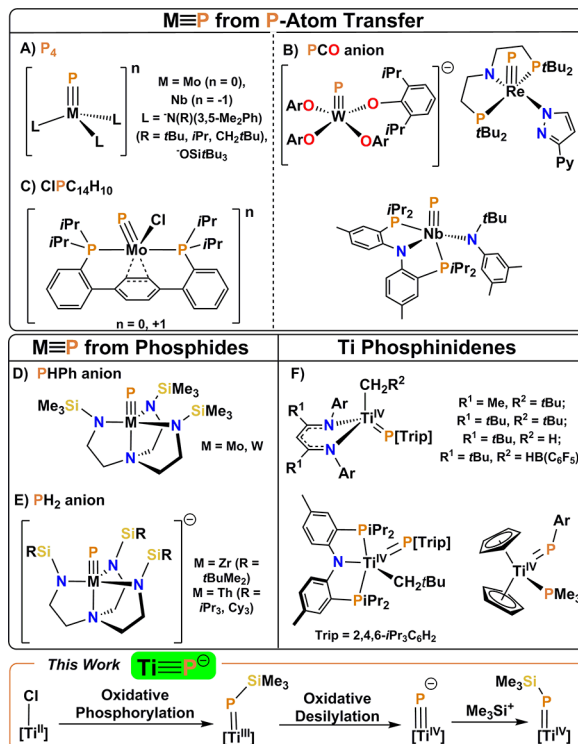


**Figure 1.** Pathways to metal phosphide and phosphido complexes (A–E) along with examples of titanium phosphinidenes (F). Below: Our work describing the synthesis of Ti phosphinidene and phosphide complexes.

the solid state to be  $[\text{O}-\text{C}\equiv\text{P}]^-$  ( $1780 \text{ cm}^{-1}$  for bridging dimer versus  $1755 \text{ cm}^{-1}$  for the free  $[\text{OCP}]^-$ ).<sup>25</sup>

Both **2** and **3** are paramagnetic and are observed to have solution magnetic moments (Evans' method; THF- $d_8$  (**2**),  $\text{C}_6\text{D}_6$  (**3**), 300 K) of  $\mu_{\text{eff}} = 2.41(2) \mu_{\text{B}}$  (**2**) and  $\mu_{\text{eff}} = 1.96(1) \mu_{\text{B}}$  (**3**), consistent with a  $d^2$ ,  $S = 1$  high-spin  $\text{Ti}^{\text{II}}$  ion and  $d^1$ ,  $S = 1/2$   $\text{Ti}^{\text{III}}$  ion, respectively.<sup>39,44–46</sup> Further evidence for these assignments was made utilizing HFEPR spectroscopy (**2**; Figure 3C) and CW-X-band EPR (**3**; Figure 3D). Compound **2** exhibited a characteristic spin triplet pattern (powder, 10 K, 212 GHz, Figure 3). The spectrum was simulated using  $S = 1$  spin Hamiltonian parameters:  $D = +2.065(5) \text{ cm}^{-1}$ ,  $E = +0.125(3) \text{ cm}^{-1}$ , and  $g = [1.965(2), 1.952(2), \text{ and } 1.999(2)]$  (Figure 3C). Despite the low symmetry of **2**, the electronic system is nearly axial ( $E/D = 0.06$ ;  $g_x \approx g_y$ , therefore  $g_{\perp} = 1.9595(10)$ ), which is in good agreement with that of the starting material **1** and the previously reported  $[\text{K(crypt)}][(\text{PN})_2\text{Ti}(\text{NCO})]$ .<sup>35,37</sup> Despite this apparent similarity,  $D$  of **1** ( $D = 2.137 \text{ cm}^{-1}$ ), **2**, and  $[\text{K(crypt)}][(\text{PN})_2\text{Ti}(\text{NCO})]$  ( $D =$

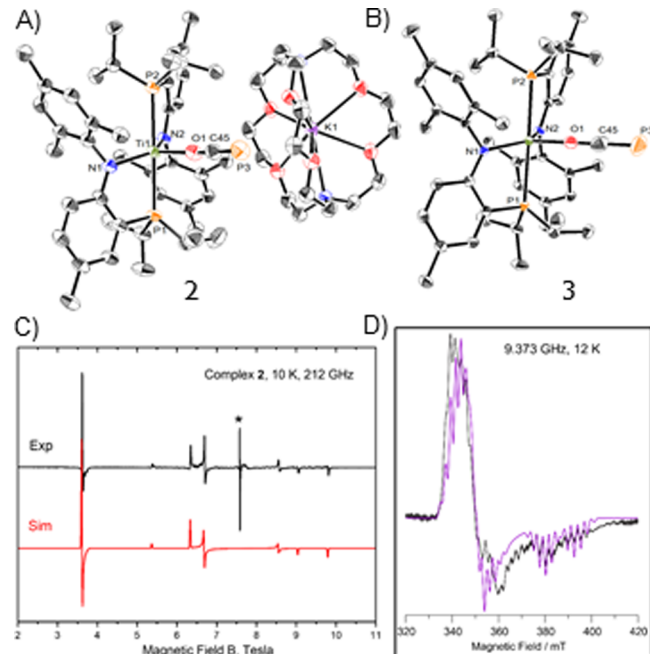


**Figure 3.** Solid state structures (ORTEP-III 50% probability) of **2** (A) and **3** (B) are shown with hydrogen and residual solvents omitted for clarity. C: HFEPR spectrum of **2** (212 GHz, 10 K; black trace) and its simulation (red trace; see text). The resonances appearing at  $\sim 7.5 \text{ T}$  (\*) correspond to an  $\text{Ti}^{\text{III}}$  impurity ( $g \sim 1.96$ ) and an unidentified radical ( $g \sim 2.00$ ) which are not simulated. D: CW-X-Band EPR spectrum (9.373 GHz, 12 K) of **3** (black trace) and its simulation (purple trace), representing the sum of two components (conformations) in equal abundance with slightly different spin Hamiltonian parameters.<sup>48</sup>

$1.967 \text{ cm}^{-1}$ ) deviate significantly, indicating differing degrees of  $\sigma$ -donation and  $\pi$ -acceptance with  $[\text{NCO}]^-$  being a stronger field ligand.<sup>35,37</sup> Given these differences,  $[\text{OCP}]^-$  spectroscopically exhibits pseudohalide characteristics; therefore, **2** appears to have more electronic similarities to **1** than  $[\text{K(crypt)}][(\text{PN})_2\text{Ti}(\text{NCO})]$ . CW-X-band EPR of **3** (9.373 GHz, 50 K, glassy toluene; Figure 3D) revealed a highly axial system, which was modeled by two conformations each with super hyperfine coupling (hfc) to two  $^{14}\text{N}$  and two  $^{31}\text{P}$  atoms.<sup>47,48</sup>

Remarkably, reduction of **3** with  $\text{KC}_8$  and cryptand also failed to promote decarbonylation but, instead, reforms **2** in 77% yield (Figure 2) in contrast to previous observations with Sc where reduction leads to P–P bond formation without decarbonylation.<sup>49</sup> Likewise, subjecting **2** or **3** to thermal and photolytic conditions does not lead to decarbonylation or formation of the target molecule:  $\text{Ti}\equiv\text{P}$  or any titanium based P-coupled product.<sup>58</sup> With the reductive decarbonylation of

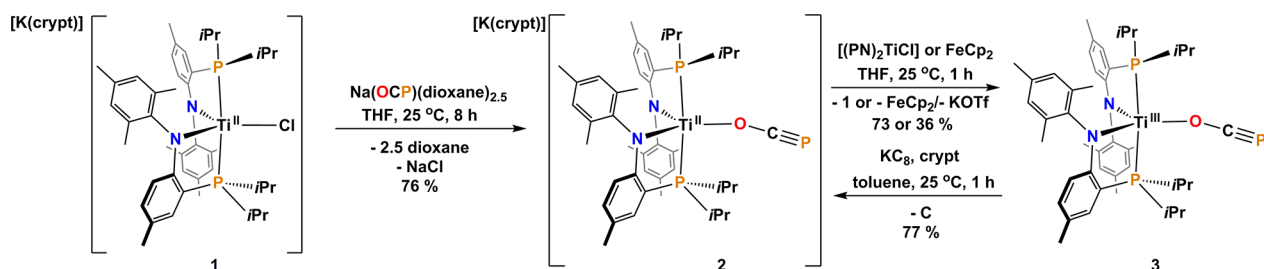


**Figure 2.** Reactivity studies involving complex **1** and  $[\text{Na(OCP)}]$  to form complex **2** and oxidized **3**.

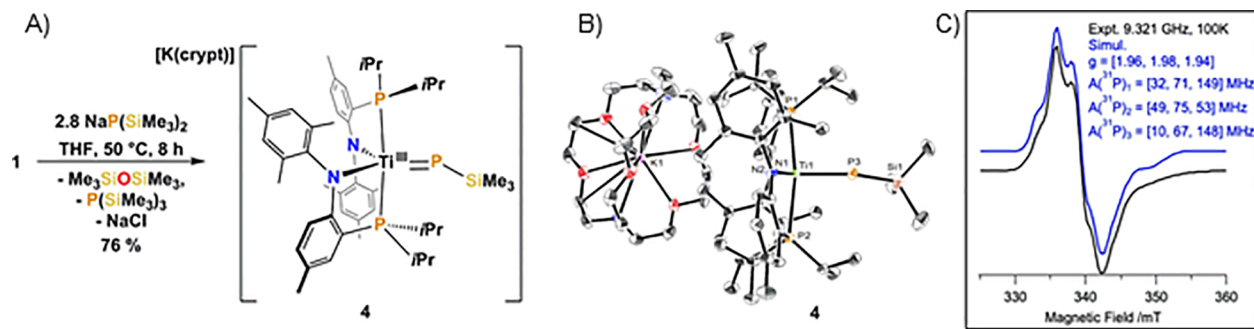


**Figure 4.** A: Reaction scheme of **1** and  $[\text{NaP}(\text{SiMe}_3)_2]$  to form the  $\text{Ti}^{\text{III}}$  phosphinidene **4** via oxidative phosphorylation. B: ORTEP-III (50% thermal ellipsoid probability) for **4** with hydrogens and residual solvents omitted. C: CW-X-band EPR (9.321 GHz, 100 K) of **4** (black) in glassy toluene and its simulation (blue) including hyperfine coupling to three  $^{31}\text{P}$  atoms.

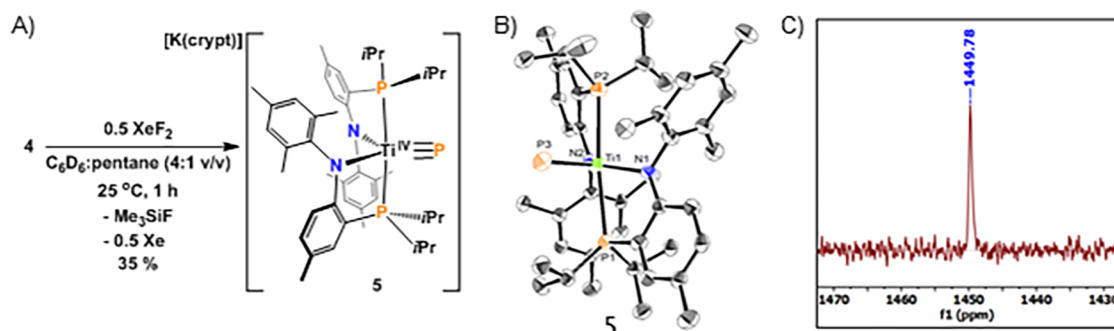


**Figure 5.** A: Reaction scheme of **4** to **5** was via oxidative desilylation. B: ORTEP-III (50% probability thermal ellipsoid) of **5**. All hydrogens,  $K(\text{crypt})$  counteranion, and cocrystallized solvent molecules have been omitted for clarity. C: Room temperature ( $300 \text{ K}$ )  $^{31}\text{P}\{^1\text{H}\}$  NMR spectrum of **5** in  $\text{THF}-d_8$ .

[OCP]<sup>-</sup> stalled, we sought an alternative method for the synthesis of  $[\text{Ti}=\text{P}]^-$ : Phosphide desilylation.

Deprotection of M=PR has been previously reported with W<sup>17</sup> and Mo<sup>18</sup> utilizing LiPHPh or LiP(SiMe<sub>3</sub>)<sub>2</sub> in which a phosphinidene intermediate was either isolated or proposed (Figure 1D). Deprotonation of M=PH has also been an effective synthetic strategy for the synthesis of terminal (Nb)<sup>19</sup> and bridging phosphide (U, Th)<sup>50–52</sup> moieties (Figure 1E). While much of the early work on group 4 M=PR was conducted on Zr,<sup>53–57</sup> such species with Ti are known, however, bulky R groups (Figure 1F) appear to be required for synthesis of the Ti=PR moiety.<sup>58–63</sup>

Complex **1** was heated and stirred at  $50^\circ\text{C}$  in THF for 8 h in the presence of an excess (2.8 equiv) of  $[\text{NaP}(\text{SiMe}_3)_2]$  to yield  $[\text{K}(\text{crypt})][\text{(PN)}_2\text{Ti}=\text{PSiMe}_3]$  (**4**) in 76% yield (Figure 4A). The scXRD study (Figure 4B) revealed a  $\text{Ti}=\text{P}$  bond length of  $2.3239(8)$  Å, which is  $\sim 0.15$  Å longer than previously reported  $\text{Ti}=\text{P}$  bond lengths ( $2.1572(2)$ – $2.2066(4)$  Å)<sup>58–63</sup> and consistent with an increased  $\text{Ti}^{\text{III}}$  ionic radius.<sup>64,65</sup> However, the  $\text{Ti}=\text{P}$  bond length in **4** is shorter than that reported by Hering-Junghans,<sup>58</sup> and the  $\angle \text{Ti}=\text{P}=\text{Si}$  bond angle of  $145.22(3)^\circ$  implies more double bond character unlike that for isoelectronic  $[\text{V}=\text{O}]^{2+}$  systems<sup>66,67</sup> and  $[\text{Ti}^{\text{III}}=\text{NR}]^+$  systems.<sup>64,65</sup>

Monitoring the progress of the reaction by NMR spectroscopy ( $^1\text{H}$ ,  $^{31}\text{P}$ , and  $^{29}\text{Si}$ -INEPT) revealed resonances attributed to unreacted  $[\text{NaP}(\text{SiMe}_3)_2]$ ,  $\text{P}(\text{SiMe}_3)_3$ , and  $\text{O}(\text{SiMe}_3)_2$ . The observed loss of  $\text{P}(\text{SiMe}_3)_3$  is similar to the reactivity reported by Scheer and Schrock for the synthesis of a W=P moiety from LiP(SiMe<sub>3</sub>)<sub>2</sub>.<sup>17,18,21</sup> Based on their mechanism, we hypothesize that the generated highly reactive  $\text{NaSiMe}_3$

reacts with O-sources by forming  $\text{O}(\text{SiMe}_3)_2$ . This unique oxidative phosphorylation is likely the result of the weak P-Si bond strength (86.9 kcal/mol) as a similar transformation is not observed between  $[\text{NaN}(\text{SiMe}_3)_2]$  with **1** (N-Si BDE 113.1 kcal/mol).<sup>64,65,67</sup>

Complex **4** shows a  $\mu_{\text{eff}} = 1.89 \mu_B$  (Evans' method,  $\text{C}_6\text{D}_6$ ,  $300 \text{ K}$ ) consistent with an  $S = 1/2$ ,  $d^1$  system,<sup>31,32,37,44–46</sup> and the CW-X-band EPR (glassy toluene; Figure 4C) revealed a spectrum modeled as an  $S = 1/2$  system with  $g$  values of  $[1.96, 1.98, 1.94]$  and super hfc to three  $^{31}\text{P}$  atoms (Figure 4C). This relatively isotropic EPR spectrum is in stark contrast to complex **3**, which shows highly axial symmetry (Figure 3D). Also notable is that complex **4** is X-band EPR-visible at  $100 \text{ K}$ , whereas **3** requires temperatures below  $77 \text{ K}$ . This EPR spectral difference might be a manifestation of the flexible Ti-OCP versus the more rigid  $\text{Ti}=\text{PSiMe}_3$  moiety.

With **4** in hand, we sought a methodology involving cleavage of the second P-Si linkage and concomitant oxidation of  $\text{Ti}^{\text{III}}$  to form a  $\text{Ti}^{\text{IV}}=\text{P}$  triple bond invoking a net loss of  $\cdot\text{SiMe}_3$ . Reaction of **4** with 0.5 eq of solid  $\text{XeF}_2$  in 4:1 (v/v)  $\text{C}_6\text{D}_6$  and pentane revealed the formation of  $\text{Me}_3\text{SiF}$  evidenced by  $^{19}\text{F}\{^1\text{H}\}$  and  $^1\text{H}$  NMR spectroscopy,<sup>69</sup> and the precipitation of a pink solid identified to be  $[\text{K}(\text{crypt})][\text{(PN)}_2\text{Ti}=\text{P}]$  (**5**), in moderate yield (35%), by scXRD and  $^1\text{H}$  and  $^{31}\text{P}\{^1\text{H}\}$  NMR spectroscopies (Figure 5A–C). This reaction involves an oxidative deprotection – here an oxidative desilylation, and such a transformation is rare for the formation of transition metal–ligand multiple bonds.<sup>64,70–74</sup> In fact, the same methodology failed when attempted for our previously reported mononuclear  $\{\text{Ti}^{\text{III}}=\text{NSiMe}_3\}^+$ , likely partially due to the increased strength of the N-Si vs P-Si bond (*vide*

*supra*).<sup>75</sup> A similar strategy for breaking P–Si bonds was reported using  $(i\text{Bu})_3\text{PAGX}$  ( $\text{X} = \text{Cl}, \text{I}$ ) by Ponikiewski for the synthesis of titanium phosphanylphosphinidene complexes ( $\text{Ti}(\eta^2\text{-PPR}_2)$ ).<sup>70</sup>

The scXRD study of **5** (Figure 5B) revealed a  $\text{Ti}\equiv\text{P}$  bond length of  $2.195(2)$  Å, which is nearly identical with the  $\text{Nb}\equiv\text{P}$  bond length of  $2.194(9)$  Å<sup>24</sup> reported by our group and other  $\text{M}\equiv\text{P}$  bond lengths reported by Cummins ( $\text{M} = \text{Nb}$ ,  $2.186(2)$  Å)<sup>14</sup> and Schrock ( $\text{M} = \text{W}$ ,  $2.162(4)$  Å).<sup>17</sup> The  $\text{Ti}\equiv\text{P}$  bond length in **5** falls between the other two reported isostructural  $[(\text{PN})_2\text{Ti}\equiv\text{E}]^-$  ( $\text{E} = \text{N}, \text{P}, \text{As}$ ) of  $1.719(3)$  Å and  $2.2661(5)$  Å for  $\text{N}^{3-}$  and  $\text{As}^{3-}$ , respectively.<sup>31,32</sup> Complex **5** represents a unique example both of a group 4 metal complex containing a metal–phosphorus triple bond and a first-row transition metal phosphide.<sup>76</sup>

The solid state structure of **5** persists in solution as confirmed by  $^1\text{H}$  NMR spectroscopy ( $\text{THF}-d_8$ ,  $300$  K), which is quite similar to the previously reported  $[\text{K}(\text{crypt})]^-[(\text{PN})_2\text{Ti}\equiv\text{E}]$  discrete salt complexes.<sup>31,32</sup> The  $^{31}\text{P}\{^1\text{H}\}$ -NMR spectrum ( $\text{THF}-d_8$ ,  $300$  K) of **5** revealed two resonances: A remarkably downfield resonance at  $\delta$   $1449.8$  ( $\nu_{1/2} = 104.2$  Hz, Figure 5C) assigned to the  $\text{Ti}\equiv\text{P}$  phosphorus and a more upfield resonance at  $\delta$   $21.7$  assigned to the equivalent PN phosphorus atoms.<sup>23,32</sup> The next furthest downfield chemical shifts for  $\text{M}\equiv\text{P}$  systems are Agapie's  $(\text{P}_2)\text{Mo}^{\text{IV}}\equiv\text{P}$  (Figure 1C)<sup>23</sup> complex and Schrock's  $(\text{N}_3\text{N})\text{-Mo}^{\text{VI}}\equiv\text{P}$  (Figure 1D),<sup>17,18</sup> which display phosphido  $^{31}\text{P}$  resonances at  $1300$  and  $1346$  ppm, respectively, whereas most others fall in the  $1000$ – $1250$  ppm range.<sup>11,13</sup>–<sup>22,72,73</sup> The large downfield  $^{31}\text{P}$  chemical shift for terminal  $\text{M}\equiv\text{P}$  systems has been attributed to the breaking of the  $C_\infty$  symmetry of the  $\text{M}\equiv\text{P}$  unit by the ligands creating systems with lower, but axial, symmetry.<sup>73</sup> Judging from previous MAS  $^{15}\text{N}$  NMR spectra for the isostructural  $[\text{K}(\text{crypt})]^-[(\text{PN})_2\text{Ti}\equiv^{15}\text{N}]$ , we expect **5** also to possess a highly axial symmetry and a large CSA.<sup>77</sup> The  $^{31}\text{P}$  chemical shift of **5** is the farthest downfield chemical shift of any terminal  $\text{M}\equiv\text{P}$  reported, likely indicating that **5** contains a highly deshielded and electron deficient P atom.

With the addition of one drop (excess) of  $\text{Me}_3\text{SiCl}$  to **5** in  $\text{THF}-d_8$ , an immediate color change from pink to dark red-orange is observed. The  $^{31}\text{P}\{^1\text{H}\}$  NMR spectrum in  $\text{THF}-d_8$  reveals the presence of a new resonance at  $\delta$   $633.5$  ( $\nu_{1/2} = 86$  Hz) as well as a doublet at  $28.4$  ( $J_{\text{P-P}} = 24$  Hz) assigned to a Ti phosphinidene and the PN ligand, respectively. Upon reaction workup, the new complex was identified to be  $[(\text{PN})_2\text{Ti}=\text{PSiMe}_3]$  (**6**, Figure 6). The downfield chemical shift in **6** is most comparable with  $[\text{Cp}_2\text{M}=\text{PR}(\text{PMMe}_3)]$  ( $\text{M} = \text{Ti}$ ,<sup>58,59</sup>  $\text{Zr}$ ,<sup>53,56</sup>  $\text{Hf}$ ,<sup>78</sup>) complexes and identical chemical shifts can also be observed upon oxidation of **4** with  $0.5$  eq of  $1,2$ -diiodoethane.<sup>79</sup> However, preparing the  $\text{Ti}^{\text{IV}}$  phosphinidene complex from **5** provides significantly higher yields than that from **4**.<sup>80</sup> Lastly, the scXRD of **6** revealed a  $\text{Ti}=\text{P}$  bond length of  $2.2388(8)$  Å, which is a contraction of  $\sim 0.08$  Å compared to that of **4** ( $2.3239(8)$  Å) and likely due to the decreased size of the  $\text{Ti}^{\text{IV}}$  ion as compared to  $\text{Ti}^{\text{III}}$ , consistent with  $\text{Ti}^{\text{IV/III}}\equiv\text{NR}$  complexes.<sup>65</sup> Complex **6** has a  $\text{Ti}=\text{P}$  bond length comparable to previously reported  $\text{Ti}=\text{PR}$  systems as well as to **4**.<sup>58,61</sup>–<sup>63</sup>

Pauling bond order calculations<sup>81</sup> utilizing the Schomaker–Stevenson correction<sup>82</sup> and the covalent radii derived from Pyykkö<sup>83</sup>–<sup>86</sup> corroborate the experimentally observed bond orders based on scXRD and  $^{31}\text{P}\{^1\text{H}\}$  NMR spectroscopy of triple for **5** and double for **4** and **6**. The calculations predict the

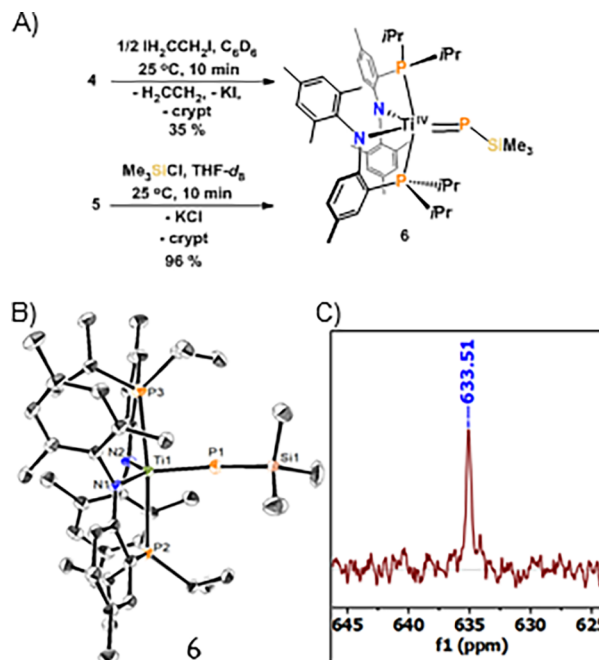


**Figure 6.** Top: Reaction scheme to form **6**. Bottom Left: ORTEP-III (50% thermal ellipsoid probability) of **6**. All hydrogens and cocrystallized solvents have been omitted. Bottom Right: Room temperature (300 K)  $^{31}\text{P}\{^1\text{H}\}$  NMR spectrum of complex **6** in  $\text{THF}-d_8$ .

$\text{Ti}=\text{P}$  bond distances of  $2.276$  and  $2.206$  Å for double and triple bond character, respectively. Therefore, we conclude that **5** clearly has a triple bond as the experimental bond distance ( $2.195(2)$  Å) is less than the predicted value, whereas phosphinidenes **4** and **6** may have some triple bond character but significantly less than those previously reported by our group (*vide supra*).<sup>61</sup>–<sup>63</sup>

In this study, we demonstrated how  $[\text{NaP}(\text{SiMe}_3)_2]$  is a more effective P atom transfer reagent than  $[\text{Na(OCP)}]$ , to synthesize a unique  $\text{Ti}^{\text{III}}$  phosphinidene as well as a one-coordinate and highly deshielded phosphide bound to  $\text{Ti}^{\text{IV}}$ . With these new methods in hand, we have made significant progress on the isostructural series of  $[(\text{PN})_2\text{Ti}\equiv\text{E}]^-$  ( $\text{E} = \text{N}, \text{P}$ , or  $\text{As}$ ) and can now begin comparing their bonding properties and reactivity.

## ASSOCIATED CONTENT

### Supporting Information

The Supporting Information is available free of charge at <https://pubs.acs.org/doi/10.1021/jacs.4c12242>.

All relevant preparation procedures and characterization data including  $^1\text{H}$ ,  $^{31}\text{P}$ ,  $^{19}\text{F}$ ,  $^{29}\text{Si}$ , and  $^{13}\text{C}$  NMR, IR, UV-vis, EPR, and scXRD data for compounds **2**–**6** (PDF)

### Accession Codes

Deposition Numbers 2380961–2380965 contain the supplementary crystallographic data for this paper. These data can be obtained free of charge via the joint Cambridge Crystallographic Data Centre (CCDC) and Fachinformationszentrum Karlsruhe Access Structures service.

## AUTHOR INFORMATION

### Corresponding Author

Daniel J. Mindiola — Department of Chemistry, University of Pennsylvania, Philadelphia, Pennsylvania 19104, United States; [orcid.org/0000-0001-8205-7868](https://orcid.org/0000-0001-8205-7868); Email: [mindiola@sas.upenn.edu](mailto:mindiola@sas.upenn.edu)

### Authors

Jacob S. Mohar — Department of Chemistry, University of Pennsylvania, Philadelphia, Pennsylvania 19104, United States

Mrinal Bhunia — Department of Chemistry, University of Pennsylvania, Philadelphia, Pennsylvania 19104, United States; [orcid.org/0000-0002-4441-9052](https://orcid.org/0000-0002-4441-9052)

Alexander L. Laughlin — Department of Chemistry and Chemical Biology, Baker Laboratory, Cornell University, Ithaca, New York 14850, United States

Andrew Ozarowski — National High Magnetic Field Laboratory, Florida State University, Tallahassee, Florida 32310, United States; [orcid.org/0000-0001-6225-9796](https://orcid.org/0000-0001-6225-9796)

J. Krzystek — National High Magnetic Field Laboratory, Florida State University, Tallahassee, Florida 32310, United States; [orcid.org/0000-0001-6088-1936](https://orcid.org/0000-0001-6088-1936)

Taylor M. Keller — Department of Chemistry, University of Pennsylvania, Philadelphia, Pennsylvania 19104, United States

Michael R. Gau — Department of Chemistry, University of Pennsylvania, Philadelphia, Pennsylvania 19104, United States; [orcid.org/0000-0002-4790-6980](https://orcid.org/0000-0002-4790-6980)

Kyle M. Lancaster — Department of Chemistry and Chemical Biology, Baker Laboratory, Cornell University, Ithaca, New York 14850, United States; [orcid.org/0000-0001-7296-128X](https://orcid.org/0000-0001-7296-128X)

Joshua Telser — Department of Biological, Physical and Health Sciences, Roosevelt University, Chicago, Illinois 60605, United States; [orcid.org/0000-0003-3307-2556](https://orcid.org/0000-0003-3307-2556)

Complete contact information is available at:

<https://pubs.acs.org/10.1021/jacs.4c12242>

### Funding

D.J.M. thanks the U.S. National Science Foundation (NSF; grants CHE-2154620, CHE-1152123, and MCB-1908587) and the University of Pennsylvania for funding. K.M.L. thanks the NSF (grant CHE-2247818) for funding. Some EPR data were obtained at ACERT, which is supported by the National Institute of General Medical Sciences of the National Institutes of Health under Award Number 1R24GM146107. A portion of this work was performed at the National High Magnetic Field Laboratory, which is supported by the NSF (Cooperative Agreement No. DMR-2128556) and the State of Florida. J.T. thanks Prof. Brian M. Hoffman, Northwestern University, for use of X- and Q-band CW EPR spectrometers, which are supported by the NSF (grant CHE-2333907).

### Notes

The authors declare no competing financial interest.

## ACKNOWLEDGMENTS

We thank Jun Gu and Chad Lawrence for insightful discussions and some assistance in NMR spectral data collection.

## ABBREVIATIONS

LiPPh, lithium phenyl phosphide; P<sub>4</sub>, white phosphorus; scXRD, single crystal X-ray diffraction; NaOCP, sodium phosphaethynolate; [A], dibenzo-7-*A*<sup>3</sup>-phosphanorbornadiene; NaOCAs, sodium arsaethynolate; THF, tetrahydrofuran; h, hours; HSAB, hard and soft acid base; NMR, nuclear magnetic resonance; MAS, magic angle spinning; EPR, electron paramagnetic resonance; HFEPR, high-frequency and -field EPR; zfs, zero-field splitting; DME, dimethoxyethane; OTf, triflate; PN, *N*-(2-(di-*iso*-propylphosphanyl)-4-methylphenyl)-2,4,6-trimethylanilide; crypt, 4,7,13,16,21,24-hexaoxa-1,10-diazabicyclo[8.8.8]hexacosane (2.2.2-cryptand); eq, equivalent (molar); INEPT, insensitive nuclei enhanced by polarization transfer; tBu, *tert*-butyl; iPr, *iso*-propyl; hfc, hyperfine coupling; PNP, bis(2-(di-*iso*-propylphosphanyl)-4-methylphenyl)-amide; Trip, 2,4,6-tri-*iso*-propylphenyl; BDI, 1,3-diketiminide; Cp, cyclopentadienyl; P<sub>n</sub>, pnictides or pnictido; N<sub>3</sub>N, [(Me<sub>3</sub>SiNCH<sub>2</sub>CH<sub>2</sub>)<sub>3</sub>N]<sup>3-</sup> (trisamido amine); P<sub>2</sub>, 2,2'-bis(di-*iso*-propylphosphanyl)-1,1':4',1"-terphenyl; CSA, Chemical Shift Anisotropy

## REFERENCES

- (1) Mohammad, A.; Alireza, K.; Mohammadreza, E. Methods and Devices Using Tri-Transition Metal Phosphides for Efficient Electrocatalytic Reactions. United States US2022154354A1, 2019.
- (2) Liu, S.; Feng, J.; Bian, X.; Liu, J.; Xu, H.; An, Y. A controlled red phosphorus@Ni-P core@shell nanostructure as an ultralong cycle-life and superior high-rate anode for sodium-ion batteries. *Energy & Environ. Sci.* **2017**, *10*, 1222–1233.
- (3) Ihsan-Ul-Haq, M.; Huang, H.; Cui, J.; Yao, S.; Wu, J.; Chong, W. G.; Huang, B.; Kim, J.-K. Chemical interactions between red P and functional groups in NiP<sub>3</sub>/CNT composite anodes for enhanced sodium storage. *J. Mater. Chem. A* **2018**, *6*, 20184–20194.
- (4) Luo, Z.-Z.; Zhang, Y.; Zhang, C.; Tan, H. T.; Li, Z.; Abutaha, A.; Wu, X.-L.; Xiong, Q.; Khor, K. A.; Hippalgaonkar, K.; Xu, J.; Hng, H. H.; Yan, Q. Multifunctional 0D–2D Ni<sub>2</sub>P Nanocrystals–Black Phosphorus Heterostructure. *Adv. Energy Mater.* **2017**, *7*, 1601285.
- (5) Wang, X.; Kim, H.-M.; Xiao, Y.; Sun, Y.-K. Nanostructured metal phosphide-based materials for electrochemical energy storage. *J. Mater. Chem. A* **2016**, *4*, 14915–14931.
- (6) Shi, Y.; Zhang, B. Recent advances in transition metal phosphide nanomaterials: synthesis and applications in hydrogen evolution reaction. *Chem. Soc. Rev.* **2016**, *45*, 1529–1541.
- (7) Cheng, Z.; Zhang, X.; Zhang, H.; Liu, H.; Yu, X.; Dai, X.; Liu, G.; Chen, G. Ti<sub>2</sub>P monolayer as a high performance 2-D electrode material for ion batteries. *Phys. Chem. Chem. Phys.* **2020**, *22*, 18480–18487.
- (8) Woo, S.-g.; Jung, J.-H.; Kim, H.; Kim, M. G.; Lee, C. K.; Sohn, H.-J.; Cho, B. W. Electrochemical Characteristics of Ti–P Composites Prepared by Mechanochemical Synthesis. *J. Electrochem. Soc.* **2006**, *153*, A1979.
- (9) Zhou, F.; Yang, X.-S.; Liu, J.; Liu, J.; Hu, R.; Ouyang, L.; Zhu, M. Boosted lithium storage cycling stability of TiP<sub>2</sub> by in-situ partial self-decomposition and nano-spatial confinement. *J. Power Sources* **2021**, *485*, No. 229337.
- (10) Zhou, F.; Liu, L.; Huang, Z.; Luo, M.; Gao, X.; Guo, S.; Ma, Z.; Li, P.; Nan, J. Constructing Multiphase Structures to Enhance Lithium Storage Performance of Black Phosphorus–Carbon Composite. *Energy Technology* **2023**, *11*, 2300387.
- (11) Laplaza, C. E.; Davis, W. M.; Cummins, C. C. A Molybdenum–Phosphorus Triple Bond: Synthesis, Structure, and Reactivity of the Terminal Phosphido (P<sup>3-</sup>) Complex [Mo(P)(NR<sub>2</sub>)<sub>3</sub>]. *Angew. Chem., Int. Ed. Engl.* **1995**, *34*, 2042–2044.
- (12) Cherry, J.-P. F.; Stephens, F. H.; Johnson, M. J. A.; Diaconescu, P. L.; Cummins, C. C. Terminal Phosphide and Dinitrogen

- Molybdenum Compounds Obtained from Pnictide-Bridged Precursors. *Inorg. Chem.* **2001**, *40*, 6860–6862.
- (13) Stephens, F. H.; Figueroa, J. S.; Diaconescu, P. L.; Cummins, C. C. Molybdenum–Phosphorus Triple Bond Stabilization by Ancillary Alkoxide Ligation: Synthesis and Structure of a Terminal Phosphide Tris-1-methylcyclohexanoxide Complex. *J. Am. Chem. Soc.* **2003**, *125*, 9264–9265.
- (14) Figueroa, J. S.; Cummins, C. C. Diorganophosphanylphosphidines as Complexed Ligands: Synthesis via an Anionic Terminal Phosphide of Niobium. *Angew. Chem., Int. Ed.* **2004**, *43*, 984–988.
- (15) Fox, A. R.; Clough, C. R.; Piro, N. A.; Cummins, C. C. A Terminal Nitride-to-Phosphide Conversion Sequence Followed by Tungsten Phosphide Functionalization Using a Diphenylphosphine Synthon. *Angew. Chem., Int. Ed.* **2007**, *46*, 973–976.
- (16) Joost, M.; Transue, W. J.; Cummins, C. C. Terminal tungsten pnictide complex formation through pnictaethynolate decarbonylation. *Chem. Commun.* **2017**, *53*, 10731–10733.
- (17) Zanetti, N. C.; Schrock, R. R.; Davis, W. M. Monomeric Molybdenum and Tungsten Complexes That Contain a Metal–Phosphorus Triple Bond. *Angew. Chem., Int. Ed. Engl.* **1995**, *34*, 2044–2046.
- (18) Mösch-Zanetti, N. C.; Schrock, R. R.; Davis, W. M.; Wanninger, K.; Seidel, S. W.; O’Donoghue, M. B. Triamidoamine Complexes of Molybdenum and Tungsten That Contain Metal–E (E = N, P, and As) Single, Double, or Triple Bonds. *J. Am. Chem. Soc.* **1997**, *119*, 11037–11048.
- (19) Hirsekorn, K. F.; Veige, A. S.; Wolczanski, P. T. PC Bond Cleavage of (silox)<sub>3</sub>NbPMe<sub>3</sub> (silox = tBu<sub>3</sub>SiO) under Dihydrogen Leads to (silox)<sub>3</sub>NbCH<sub>2</sub>, (silox)<sub>3</sub>NbPH or (silox)<sub>3</sub>NbP(H)Nb-(silox)<sub>3</sub>, and CH<sub>4</sub>. *J. Am. Chem. Soc.* **2006**, *128*, 2192–2193.
- (20) Kuiper, D. S.; Wolczanski, P. T.; Lobkovsky, E. B.; Cundari, T. R. Low Coordinate, Monomeric Molybdenum and Tungsten(III) Complexes: Structure, Reactivity and Calculational Studies of (silox)<sub>3</sub>Mo and (silox)<sub>3</sub>ML (M = Mo, W; L = PMe<sub>3</sub>, CO; silox = tBu<sub>3</sub>SiO). *J. Am. Chem. Soc.* **2008**, *130*, 12931–12943.
- (21) Scheer, M.; Müller, J.; Häser, M. Complexes Containing Phosphorus and Arsenic as Terminal Ligands. *Angew. Chem., Int. Ed. Engl.* **1996**, *35*, 2492–2496.
- (22) Abbenseth, J.; Diefenbach, M.; Hinz, A.; Alig, L.; Würtele, C.; Goicoechea, J. M.; Holthausen, M. C.; Schneider, S. Oxidative Coupling of Terminal Rhodium Pnictide Complexes. *Angew. Chem., Int. Ed.* **2019**, *58*, 10966–10970.
- (23) Buss, J. A.; Oyala, P. H.; Agapie, T. Terminal Molybdenum Phosphides with d Electrons: Radical Character Promotes Coupling Chemistry. *Angew. Chem., Int. Ed.* **2017**, *56*, 14502–14506.
- (24) Senthil, S.; Kwon, S.; Fehn, D.; Im, H.; Gau, M. R.; Carroll, P. J.; Baik, M.-H.; Meyer, K.; Mindiola, D. J. Metal-Ligand Cooperativity to Assemble a Neutral and Terminal Niobium Phosphorus Triple Bond (Nb≡P). *Angew. Chem., Int. Ed.* **2022**, *61*, No. e202212488.
- (25) Puschmann, F. F.; Stein, D.; Heift, D.; Hendriksen, C.; Gal, Z. A.; Grützmacher, H.-F.; Grützmacher, H. Phosphination of Carbon Monoxide: A Simple Synthesis of Sodium Phosphaethynolate (NaOCP). *Angew. Chem., Int. Ed.* **2011**, *50*, 8420–8423.
- (26) Jacobs, H.; Hassiepen, K. M. Über die Dihydrogenphosphide der Alkalimetalle, MPH<sub>2</sub> mit M ≈ Li, Na, K, Rb und Cs. *Z. Anorg. Allg. Chem.* **1985**, *531*, 108–118.
- (27) Heift, D.; Benkő, Z.; Grützmacher, H. Coulomb repulsion versus cycloaddition: formation of anionic four-membered rings from sodium phosphaethynolate, Na(OCP). *Dalton Trans.* **2014**, *43*, 831–840.
- (28) Goicoechea, J. M.; Grützmacher, H. The Chemistry of the 2-Phosphaethynolate Anion. *Angew. Chem., Int. Ed.* **2018**, *57*, 16968–16994.
- (29) Transue, W. J.; Nava, M.; Terban, M. W.; Yang, J.; Greenberg, M. W.; Wu, G.; Foreman, E. S.; Mustoe, C. L.; Kenneppohl, P.; Owen, J. S.; Billinge, S. J. L.; Kulik, H. J.; Cummins, C. C. Anthracene as a Launchpad for a Phosphinidene Sulfide and for Generation of a Phosphorus–Sulfur Material Having the Composition P<sub>2</sub>S, a Vulcanized Red Phosphorus That Is Yellow. *J. Am. Chem. Soc.* **2019**, *141*, 431–440.
- (30) Velian, A.; Nava, M.; Temprado, M.; Zhou, Y.; Field, R. W.; Cummins, C. C. A retro Diels-Alder route to diphosphorus chemistry: molecular precursor synthesis, kinetics of P<sub>2</sub> transfer to 1,3-dienes, and detection of P<sub>2</sub> by molecular beam mass spectrometry. *J. Am. Chem. Soc.* **2014**, *136*, 13586–13589.
- (31) Carroll, M. E.; Pinter, B.; Carroll, P. J.; Mindiola, D. J. Mononuclear and Terminally Bound Titanium Nitrides. *J. Am. Chem. Soc.* **2015**, *137*, 8884–8887.
- (32) Bhunia, M.; Mohar, J. S.; Sandoval-Pauker, C.; Fehn, D.; Yang, E. S.; Gau, M.; Goicoechea, J.; Ozarowski, A.; Krzystek, J.; Telser, J.; Meyer, K.; Mindiola, D. J. Softer Is Better for Titanium: Molecular Titanium Arsenido Anions Featuring Ti≡As Bonding and a Terminal Parent Arsinidene. *J. Am. Chem. Soc.* **2024**, *146*, 3609–3614.
- (33) Tambornino, F.; Hinz, A.; Köppe, R.; Goicoechea, J. M. A General Synthesis of Phosphorus- and Arsenic-Containing Analogues of the Thio- and Seleno-cyanate Anions. *Angew. Chem., Int. Ed.* **2018**, *57*, 8230–8234.
- (34) Lu, Y.; Wang, H.; Xie, Y.; Liu, H.; Schaefer, H. F. The Cyanate and 2-Phosphaethynolate Anion Congeners ECO<sup>-</sup> (E = N, P, As, Sb, Bi): Prelude to Experimental Characterization. *Inorg. Chem.* **2014**, *53*, 6252–6256.
- (35) See ESI for details regarding this reaction.
- (36) Shannon, R. Revised effective ionic radii and systematic studies of interatomic distances in halides and chalcogenides. *Acta Crystallogr., Sect. A* **1976**, *32*, 751–767.
- (37) Bhunia, M.; Sandoval-Pauker, C.; Fehn, D.; Grant, L.; Senthil, S.; Gau, M.; Ozarowski, A.; Krzystek, J.; Telser, J.; Pinter, B.; Meyer, K.; Mindiola, D. J. Divalent Titanium via Reductive N-C Coupling of a Ti<sup>IV</sup> Nitrido with π-Acids. *Angew. Chem., Int. Ed.* **2024**, *136*, No. e202404601. Scott, B. A.; Eulenberger, G. R.; Bernheim, R. A. Magnetic Susceptibility and Nuclear Magnetic Resonance Studies of Transition-Metal Monophosphides. *J. Chem. Phys.* **1968**, *48*, 263–272.
- (38) Grant, L. N.; Pinter, B.; Manor, B. C.; Suter, R.; Grützmacher, H.; Mindiola, D. J. A Planar Ti<sub>2</sub>P<sub>2</sub> Core Assembled by Reductive Decarbonylation of ^O-C≡P and P–P Radical Coupling. *Chem.–Eur. J.* **2017**, *23*, 6272–6276.
- (39) Grant, L. N.; Krzystek, J.; Pinter, B.; Telser, J.; Grützmacher, H.; Mindiola, D. J. Finding a soft spot for vanadium: a P-bound OCP ligand. *Chem. Commun.* **2019**, *55*, 5966–5969.
- (40) Pearson, R. G. Hard and soft acids and bases, HSAB, part II: Underlying theories. *J. Chem. Educ.* **1968**, *45*, 643.
- (41) Pearson, R. G. Hard and soft acids and bases, HSAB, part I: Fundamental principles. *J. Chem. Educ.* **1968**, *45*, 581.
- (42) Pearson, R. G. Hard and Soft Acids and Bases. *J. Am. Chem. Soc.* **1963**, *85*, 3533–3539.
- (43) See ESI Figures S4.1.1 and S4.2.1–2 for more details.
- (44) Evans, D. F. The determination of the paramagnetic susceptibility of substances in solution by nuclear magnetic resonance. *J. Chem. Soc. (Resumed)* **1959**, 2003.
- (45) Sur, S. K. Measurement of magnetic susceptibility and magnetic moment of paramagnetic molecules in solution by high-field fourier transform NMR spectroscopy. *J. Magn. Reson.* **1989**, *82*, 169–173.
- (46) Bain, G. A.; Berry, J. F. Diamagnetic Corrections and Pascal’s Constants. *J. Chem. Educ.* **2008**, *85*, 532.
- (47) See Figure 3 caption and ESI Figures S6.1–S6.4 for details.
- (48) Each conformation includes hyperfine coupling to each of two equivalent <sup>31</sup>P and <sup>14</sup>N nuclei: (1) g = [1.960, 1.915, 1.761], A(<sup>31</sup>P) = [70, 60, 70] MHz, A(<sup>14</sup>N) = [60, 40, 60] MHz; (2) g = [1.950, 1.895, 1.706], A(<sup>31</sup>P) = [110, 120, 75] MHz, A(<sup>14</sup>N) = [55, 60, 65] MHz. These components are shown separately in Figure S6.3 along with an expansion of the g<sub>||</sub> region (Figure S6.2) and a Q-band (35 GHz) EPR spectrum (Figure S6.4). There may be a third component, not simulated, with g<sub>⊥</sub> and g<sub>||</sub> still lower: at g<sub>⊥</sub> ≈ 1.86 (~360 mT) and g<sub>||</sub> ≈ 1.63 (~410 mT), respectively.

- (49) Grant, L. N.; Pinter, B.; Manor, B. C.; Grützmacher, H.; Mindiola, D. J. A Scandium-Stabilized Diisophosphaethynolate Ligand:  $[OCPPCO]^{4-}$ . *Angew. Chem., Int. Ed.* **2018**, *57*, 1049–1052.
- (50) Wildman, E. P.; Balázs, G.; Woole, A. J.; Scheer, M.; Liddle, S. T. Thorium–phosphorus triamidoamine complexes containing Th–P single- and multiple-bond interactions. *Nat. Commun.* **2016**, *7*, 12884.
- (51) Gardner, B. M.; Balázs, G.; Scheer, M.; Tuna, F.; McInnes, E. J. L.; McMaster, J.; Lewis, W.; Blake, A. J.; Liddle, S. T. Triamidoamine–Uranium(IV)-Stabilized Terminal Parent Phosphide and Phosphinidene Complexes. *Angew. Chem., Int. Ed.* **2014**, *53*, 4484–4488.
- (52) Rookes, T. M.; Gardner, B. M.; Balázs, G.; Gregson, M.; Tuna, F.; Woole, A. J.; Scheer, M.; Liddle, S. T. Crystalline Diuranium Phosphinidide and  $\mu$ -Phosphido Complexes with Symmetric and Asymmetric UPU Cores. *Angew. Chem., Int. Ed.* **2017**, *56*, 10495–10500.
- (53) Ho, J.; Hou, Z.; Drake, R. J.; Stephan, D. W. Phosphorus-hydrogen and cyclopentadienyl carbon-hydrogen activation en route to homo- and heterobinuclear zirconocene phosphide and phosphinidene complexes. *Organometallics* **1993**, *12*, 3145–3157.
- (54) Hou, Z.; Breen, T. L.; Stephan, D. W. Formation and reactivity of the early metal phosphides and phosphinidenes  $Cp^*_2Zr:PR$ ,  $Cp^*_2Zr(PR)_2$ , and  $Cp^*_2Zr(PR)_3$ . *Organometallics* **1993**, *12*, 3158–3167.
- (55) Fermin, M. C.; Ho, J.; Stephan, D. W. Sterically Induced P-C Bond Cleavage: Routes to Substituent-Free Phosphorus Complexes of Zirconium. *Organometallics* **1995**, *14*, 4247–4256.
- (56) Kilgore, U. J.; Fan, H.; Pink, M.; Urnezius, E.; Protasiewicz, J. D.; Mindiola, D. J. Phosphinidene group-transfer with a phospho-Wittig reagent: a new entry to transition metal phosphorus multiple bonds. *Chem. Commun.* **2009**, 4521–4523.
- (57) Ho, J.; Stephan, D. W. Synthesis of zirconocene phosphinidenes and phosphides via phosphorus-hydrogen activation. *Organometallics* **1991**, *10*, 3001–3003.
- (58) Fischer, M.; Reiß, F.; Hering-Junghans, C. Titanocene pnictinidene complexes. *Chem. Commun.* **2021**, *57*, 5626–5629.
- (59) Masuda, J. D.; Hoskin, A. J.; Graham, T. W.; Beddie, C.; Fermin, M. C.; Etkin, N.; Stephan, D. W. Catalytic P-H Activation by Ti and Zr Catalysts. *Chem.—Eur. J.* **2006**, *12*, 8696–8707.
- (60) Ponikiewski, Ł.; Ziolkowska, A.; Pikies, J. Reactions of Lithiated Diphenophanes  $R_2P—P(SiMe_3)Li$  ( $R = tBu$  and  $iPr$ ) with  $[MeNacnacTiCl_2\cdot THF]$  and  $[MeNacnacTiCl_3]$ . Formation and Structure of TitaniumIII and TitaniumIV  $\beta$ -Diketiminato Complexes Bearing the Side-on Phosphanylphosphido and Phosphanylphosphinidene Functionalities. *Inorg. Chem.* **2017**, *56*, 1094–1103.
- (61) Zhao, G.; Basuli, F.; Kilgore, U. J.; Fan, H.; Aneetha, H.; Huffman, J. C.; Wu, G.; Mindiola, D. J. Neutral and Zwitterionic Low-Coordinate Titanium Complexes Bearing the Terminal Phosphinidene Functionality. Structural, Spectroscopic, Theoretical, and Catalytic Studies Addressing the Ti–P Multiple Bond. *J. Am. Chem. Soc.* **2006**, *128*, 13575–13585.
- (62) Bailey, B. C.; Huffman, J. C.; Mindiola, D. J.; Weng, W.; Ozerov, O. V. Remarkably Stable Titanium Complexes Containing Terminal Alkylidene Phosphinidene, and Imide Functionalities. *Organometallics* **2005**, *24*, 1390–1393.
- (63) Basuli, F.; Tomaszewski, J.; Huffman, J. C.; Mindiola, D. J. Four-Coordinate Phosphinidene Complexes of Titanium Prepared by  $\alpha$ -H-Migration: Phospha-Staudinger and Phosphaalkene-Insertion Reactions. *J. Am. Chem. Soc.* **2003**, *125*, 10170–10171.
- (64) Bailey, B. C.; Basuli, F.; Huffman, J. C.; Mindiola, D. J. Terminal Titanium(IV) (Trimethylsilyl)imides Prepared by Oxidatively Induced Trimethylsilyl Abstraction. *Organometallics* **2006**, *25*, 2725–2728.
- (65) Mohar, J. S.; Reinholdt, A.; Keller, T. M.; Carroll, P. J.; Telser, J.; Mindiola, D. J. A mononuclear, terminal titanium(III) imido. *Chem. Commun.* **2023**, *59*, 10101–10104.
- (66) Ballhausen, C. J.; Gray, H. B. The Electronic Structure of the Vanadyl Ion. *Inorg. Chem.* **1962**, *1*, 111–122.
- (67) Cottrell, T. L. *The strengths of chemical bonds*; Butterworths Scientific Publications, 1958.
- (68) See ESI Figures S3.7.4–6 for details.
- (69) See ESI Figures S3.5.7–9 for details.
- (70) Ziolkowska, A.; Szynkiewicz, N.; Wiśniewska, A.; Pikies, J.; Ponikiewski, Ł. Reactions of  $(Ph)BuP-P(SiMe_3)Li\cdot 3THF$  with  $[(PNP)TiCl_2]$  and  $[MeNacnacTiCl_2\cdot THF]$ : synthesis of first PNP titanium(IV) complex with the phosphanylphosphinidene ligand  $[(PNP)Ti(Cl)\{\eta^2-P-P(Ph)Bu\}]$ . *Dalton Trans.* **2018**, *47*, 9733–9741.
- (71) Mindiola, D. J. Oxidatively Induced Abstraction Reactions. A Synthetic Approach to Low-Coordinate and Reactive Early Transition Metal Complexes Containing Metal–Ligand Multiple Bonds. *Acc. Chem. Res.* **2006**, *39*, 813–821.
- (72) Figueroa, J. S.; Cummins, C. C. Phosphaalkynes from Acid Chlorides via P for O(Cl) Metathesis: A Recyclable Niobium Phosphide ( $P^3$ ) Reagent that Effects C–P Triple-Bond Formation. *J. Am. Chem. Soc.* **2004**, *126*, 13916–13917.
- (73) Johnson-Carr, J. A.; Zanetti, N. C.; Schrock, R. R.; Hopkins, M. D. Force Constants of Molybdenum-and Tungsten–Pnictogen Triple Bonds. *J. Am. Chem. Soc.* **1996**, *118*, 11305–11306.
- (74) Wu, G.; Rovnyak, D.; Johnson, M. J. A.; Zanetti, N. C.; Musaev, D. G.; Morokuma, K.; Schrock, R. R.; Griffin, R. G.; Cummins, C. C. Unusual  $^{31}P$  Chemical Shielding Tensors in Terminal Phosphido Complexes Containing a Phosphorus–Metal Triple Bond. *J. Am. Chem. Soc.* **1996**, *118*, 10654–10655.
- (75) Pauling, L. The Nature of the Chemical Bond. IV. The Energy of Single Bonds and the Relative Electronegativity of Atoms. *J. Am. Chem. Soc.* **1932**, *54*, 3570–3582.
- (76) Bhunia, M.; Mena, M. R.; Mohar, J. S.; Gau, M. R.; Mindiola, D. J. Molecular Phosphide Complexes of Zirconium. *J. Am. Chem. Soc.* **2025**, *147* (4), 2984–2990.
- (77) Grant, L. N.; Pinter, B.; Kurogi, T.; Carroll, M. E.; Wu, G.; Manor, B. C.; Carroll, P. J.; Mindiola, D. J. Molecular titanium nitrides: nucleophiles unleashed. *Chem. Sci.* **2017**, *8*, 1209–1224.
- (78) Waterman, R.; Tilley, T. D. Terminal hafnium phosphinidene complexes and phosphinidene ligand exchange. *Chem. Sci.* **2011**, *2*, 1320–1325.
- (79) See ESI Figures S3.6.8–10 for details.
- (80) See ESI Section 2.6 and Figure S3.6.10 for details.
- (81) Pauling, L. *The Nature of the Chemical Bond*; Cornell University Press, 1960.
- (82) Schomaker, V.; Stevenson, D. P. Some Revisions of the Covalent Radii and the Additivity Rule for the Lengths of Partially Ionic Single Covalent Bonds. *J. Am. Chem. Soc.* **1941**, *63*, 37–40.
- (83) Pyykkö, P.; Atsumi, M. Molecular Single-Bond Covalent Radii for Elements 1–118. *Chem.—Eur. J.* **2009**, *15*, 186–197.
- (84) Pyykkö, P.; Atsumi, M. Molecular Double-Bond Covalent Radii for Elements Li–E112. *Chem.—Eur. J.* **2009**, *15*, 12770–12779.
- (85) Pyykkö, P.; Riedel, S.; Patzschke, M. Triple-Bond Covalent Radii. *Chem.—Eur. J.* **2005**, *11*, 3511–3520.
- (86) Pyykkö, P. Additive Covalent Radii for Single-, Double-, and Triple-Bonded Molecules and Tetrahedrally Bonded Crystals: A Summary. *J. Phys. Chem. A* **2015**, *119*, 2326–2337.